Inverse energy transfer in finite-temperature superfluid vortex reconnections

P. Z. Stasiak, A. Baggaley, and C.F. Barenghi
School of Mathematics, Statistics and Physics, Newcastle University, Newcastle upon Tyne, NE1 7RU, United Kingdom

G. Krstulovic
Université Côte d'Azur, Observatoire de la Côte d'Azur, CNRS,Laboratoire Lagrangre, Boulevard de l'Observatoire CS 34229 - F 06304 NICE Cedex 4, France

L. Galantucci
Istituto per le Applicazioni del Calcolo "M. Picone" IAC CNR, Via dei Taurini 19, 00185 Roma, Italy
(Dated: January 16, 2025)

We numerically show that during a superfluid vortex reconnection energy is injected into the thermal (normal) component of helium II at small length scales, but is transferred nonlinearly to larger length scales, increasing the integral length scale of the normal fluid. We provide an explanation of this inverse energy transfer by decomposing the velocity and the mutual friction (which couples superfluid and normal fluid) into helical modes, showing that the imbalance of homochiral modes results from the punctuated energy and helicity injection during the reconnection. Crucially, the chiral imbalance occurs spontaneously from reconnections, unlike ordinary Navier-Stokes turbulence where careful external control is required. Finally, we discuss the relevance of our findings to the problem of superfluid turbulence.

[Proposed notation changes to avoid confusions: vortex collection $\mathcal{T} \to \mathcal{L}$ or $\mathcal{C}$, integral scale $\mathcal{L} \to L_0$]

Turbulence is ubiquitous in the universe. It occurs in systems as large as nebulae of interstellar gas, and as small as clouds of few thousands atoms confined by lasers in the laboratory. Turbulence shapes patterns and properties of fluids of all kinds, from ordinary viscous fluids (Navier-Stokes turbulence[1]) to electrically conducting fluids (magneto-hydrodynamics turbulence [2]) to quantum fluid (quantum turbulence [3, 4]). All turbulent systems are characterised by the existence of a wide range of length scales across which inviscid conserved quantities are transferred without loss in the spirit of the cascade depicted by Richardson [5].

In three-dimensional classical fluids, turbulence is characterised by a direct cascade: the non-linear dissipationless transfer of kinetic energy from the scale of the large eddies (at which energy is injected) to the smallest length scales at which energy is dissipated into heat [5, 6]. The resulting distribution of energy across length scales is the celebrated Kolmogorov energy spectrum [1, 6].

Confining Navier-Stokes turbulence to two-dimensions entails fundamentally distinct physics: a dual cascade emerges of energy and enstrophy (mean squared vorticity) [7, 8], the two conserved quantities in ideal two-dimensional flows. In particular, while the enstrophy cascade is direct (from large to small scales), the energy cascade is inverse (from small to large scales) [9]. This inverse cascade may favour the generation and persistence of large coherent structures [10].

Remarkably, the same cascade phenomenology is observed in turbulent flows of quantum fluids, *i.e.* fluids at very low temperatures whose physics is dominated by quantum effects. Examples of such fluids are superfluid helium and atomic Bose-Einstein Condensates (BECs). The dynamics of these systems can be successfully depicted in terms of a two-fluid model [11–13] describing the quantum fluid as the mixture of two components, the superfluid component and the thermal (or normal) component, which interact by means of a mutual friction force [14–16]. The superfluid component flows without viscosity and vanishing entropy; its vorticity is confined to effectively one-dimensional vortex filaments of atomic core thickness (called quantum vortices or vortex lines), around which the circulation of the velocity is quantised. In BECs the thermal component forms a ballistic gas, whereas in superfluid ^{4}He it can be described as a classical viscous fluid. Despite these significant differences with respect to ordinary fluids, the forward kinetic energy cascade has indeed been observed in three-dimensional superfluid turbulence [17–20] **[and PRB PRX of 3D cascade]** Ėvidence of this forward cascade has been found also in three-dimensional turbulent BECs [21]**[add wave turbulence BEC 3D]** . An inverse energy cascade characterises two-dimensional BECs, as shown in theoretical [22–24] **[PRL of 2D cascades]** and experimental [25, 26] studies.

The idea that the direction of the energy cascade is determined by the dimensionality of the flow and its invariants has been a longstanding belief. However, recent studies have demonstrated that in three-dimensional classical turbulence, the direction of the energy cascade may be controlled by governing the chirality of the flow, *i.e.* the balance between positive or negative helical modes [27] and their interactions. Indeed, by restricting

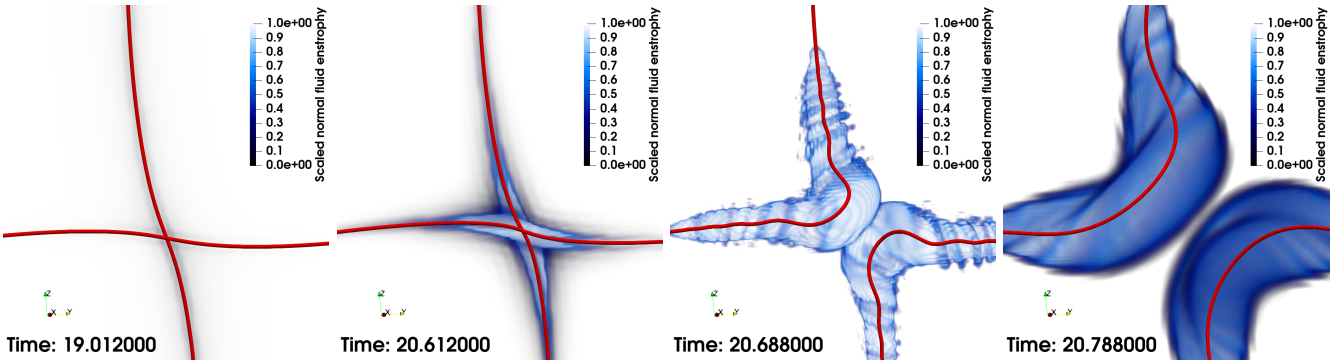

FIG. 1: Three-dimensional rendering of an orthogonal vortex configuration undergoing a vortex reconnection. The red tubes represent the superfluid vortex lines (the tubes' radii have been greatly exaggerated for visual purposes), and the blue volume rendering represents the scaled normal fluid enstrophy $\boldsymbol{\omega}^2/\boldsymbol{\omega}^2_{max}$. In the third panel, note the Kelvin waves on the superfluid vortices. **[we lack a discussion of units in the text. T =?]**

the non-linear energy transfer to homochiral interactions via a suitable decimation of the Navier-Stokes equation [28, 29], controlling the weight of homochiral interactions [30] or the external injection of positive helical modes at all length scales [31], inverse energy cascades have been observed in three-dimensional turbulence of classical fluids. In brief, when the flow is synthetically designed to have an enhanced chirality, an inverse energy cascade can observed.

In this work, we unveil a similar dynamics occurring in superfluid helium (^{4}He) as a result of vortex reconnections. Reconnections occur continuously in turbulence: they occur when two vortex lines collide and recombine, exchanging heads and tails, altering the overall topology of the flow [32–37]**[ADD PRF]**. Indeed, we show that the mutual friction force arising from the vortex reconnection is chiral, injecting in the normal fluid prevalently helicity of a given sign. Thus, as a consequence of vortex reconnections, we observe an increase of the chiral imbalance of the quantum fluid, producing a transfer of kinetic energy from small to large scales, similarly to the phenomenology observed in 3D helical-decimated classical flows. Importantly, this chiral imbalance arises naturally in the normal fluid as a result of vortex reconnections. This is contrast to classical fluid dynamics, where the helical characteristics of the flows producing an inverse energy transfer require a careful synthetic construction [28–31].

To model superfluid helium dynamics, we employ the recently developed FOUCAULT model [38]. In this approach, superfluid vortex lines are parametrized as one-dimensional space curves $\mathbf{s}(\xi, t)$, ξ and t being arclength and time respectively, exploiting the large seperation of length scales between the vortex core radius, the Lagrangian discretisation along the vortex lines $\Delta\xi$, and the average radius of curvature R_c of the vortex lines. The vortex lines evolve according to the following equation of motion:

$$\dot{\mathbf{s}}(\xi,t) = \mathbf{v}_s + \frac{\beta}{1+\beta}\left[\mathbf{v}_{ns}\cdot\mathbf{s}'\right]\mathbf{s}' + \beta\mathbf{s}'\times\mathbf{v}_{ns} + \beta'\mathbf{s}'\times\left[\mathbf{s}'\times\mathbf{v}_{ns}\right], \tag{1}$$

where $\dot{\mathbf{s}} = \partial\mathbf{s}/\partial t$, $\mathbf{s}' = \partial\mathbf{s}/\partial\xi$ is the unit tangent vector, $\mathbf{v}_n$ and $\mathbf{v}_s$ are the normal fluid and superfluid velocities at $\mathbf{s}$, $\mathbf{v}_{ns} = \mathbf{v}_n - \mathbf{v}_s$, and β, β' are temperature and Reynolds number dependent mutual friction coeffi-

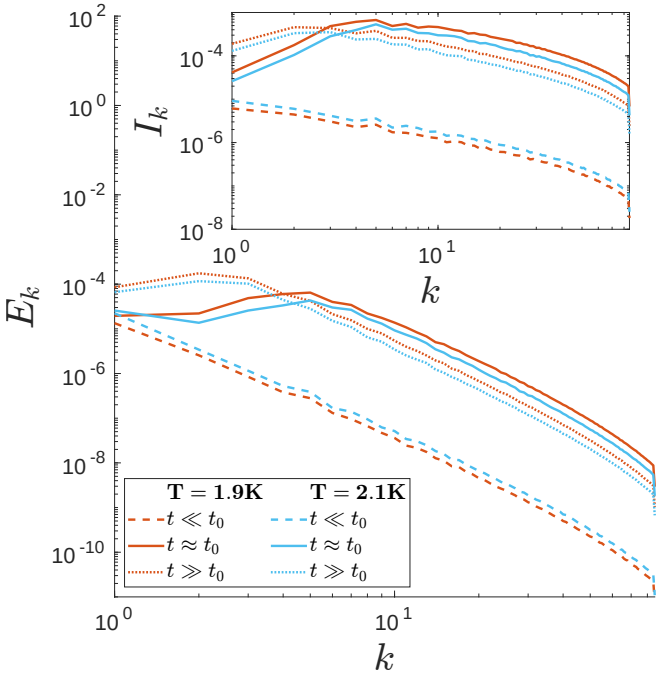

FIG. 2: Normal fluid kinetic energy spectrum $E(k)$ before reconnection (dashed lines), at reconnection (solid lines) and after reconnection (dotted lines) for $T = 1.9K$ (red) and $T = 2.1K$ (blue). *Inset:* Energy injection spectrum $I(k)$ arising from the mutual friction forcing at the same times as in the main figure.

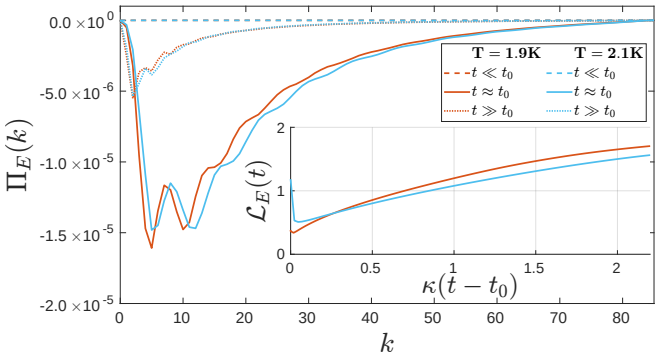

FIG. 3: *Top:* Mutual friction injection spectrum, I_k. *Bottom:* Spectral normal fluid kinetic energy flux, Π_E. *Inset:* Post reconnection evolution of the integral length scale, $\mathcal{L}_E$. Times and temperatures are labelled as in Fig. 2

.

cients [38]. The calculation of the superfluid velocity $\mathbf{v}_s$ is performed via the computation of the Biot-Savart integral de-singularised with standard techniques (see Supplementary Material [39]). The normal fluid is described classically using the incompressible ($\nabla \cdot \mathbf{v}_n = 0$) Navier-Stokes equation

$$\frac{\partial \mathbf{v}_n}{\partial t} + (\mathbf{v}_n \cdot \nabla)\mathbf{v}_n = -\frac{1}{\rho}\nabla p + \nu_n \nabla^2 \mathbf{v}_n + \frac{\mathbf{F}_{ns}}{\rho_n} \quad , \qquad (2)$$

where ρ_n and ρ_s are the normal fluid and superfluid densities, $\rho = \rho_n + \rho_s$, p is the pressure, ν_n is the kinematic viscosity of the normal fluid, and the mutual friction force per unit volume, $\mathbf{F}_{ns}$, is the line integral of the mutual friction force per unit length, $\mathbf{f}_{ns}$ [39]:

$$\mathbf{F}_{ns}(\mathbf{x}) = \oint_{\mathcal{T}} \delta(\mathbf{x} - \mathbf{s})\mathbf{f}_{ns}(\mathbf{s})d\xi, \qquad (3)$$

$\mathcal{T}$ representing the entire vortex configuration. The regularisation of mutual friction is performed using a physically self-consistent scheme [38, 40, 41].

To study the reconnection dynamics, we consider two pairs of initially orthogonal vortices (where the corresponding vortices of each pair have opposite circulation in order to preserve periodicity along the boundaries) at two temperatures, $T = 1.9K$ and $T = 2.1K$. The vortex pairs are separated by the distance D_ℓ; each vortex within each pair is initially at distance d_ℓ to the other vortex, such that $d_\ell \ll D_\ell$ to ensures that the dynamics in the vicinity of the reconnection is dominated by local interactions, and that the far-field contribution from the other vortex pair is neglible. The evolution of the vortex reconnection of a single pair is reported in Fig. 1.

We first focus the attention on the time evolution of the normal fluid energy spectrum $E(k)$ (where k is the magnitude of the three-dimensional wavenumber), illustrated in Fig. 2, where it clearly emerges that, during the reconnection, energy is predominantly injected into the normal fluid at intermediate and small length scales. For $k > 5$ in correspondence of the reconnection time t_0, we observe a significant increase of the normal fluid energy spectral density: $E(k, t \approx t_0)/E(k, t \ll t_0) \approx 10^2$.

In the post-reconnection regime, we simultaneously observe a small decrease of the spectrum at intermediate and small scales ($k > 5$) and an increase at large scales, suggesting the existence of a mechanism by which energy generated at small length scales is transferred to larger scales. To shed light on this mechanism we analyse the dynamics of the normal fluid flow using the spectral energy budget equation:

$$\frac{\partial E(k)}{\partial t} = T(k) - D(k) + I(k) \qquad (4)$$

where $T(k)$ is the spectral kinetic energy transfer function, $D(k) = 2\nu_n k^2 E_k$ is the dissipation spectrum and $I(k)$ is the injection spectrum arising from the mutual friction force $\mathbf{F}_{ns}$. Immediately after the reconnection, each vortex has the shape of a sharp cusp (corresponding to a small radius of curvature R_c) which immediately starts relaxing (R_c increases). Since $|\mathbf{F}_{ns}| \propto |\dot{\mathbf{s}} - \mathbf{v}_n| \approx |\dot{\mathbf{s}}| \propto 1/R_c$, the scales of energy injection at reconnection are necessarily much smaller than the original length scales before the reconnection, as it can be observed in the inset of Fig. 2. As time evolves, the smallest perturbations on the vortex lines are damped by friction the fastest, resulting in the shift of the peak of the injection spectrum $I(k)$ towards larger length scales. However this shift does not account for the increase of $E(k)$ at the largest scales after reconnection, which arises from non-linear effects. Indeed, if we compute the energy flux $\Pi(k) = \int_k^\infty T(k')dk'$ (reported in Fig. 3 at different times and temperatures), we observe that $\Pi(k) < 0$ for all k during and after reconnection; we also observe that, near the time of reconnection, the peak value of $|\Pi(k)|$ is in the range $5 < k < 15$. The negative sign of $\Pi(k)$ is evidence of a flux of kinetic energy from small to large scales. In other words, at non-zero temperatures, vortex reconnections trigger an inverse transfer of energy, which implies the creation of large scale structures, visible in Fig. 1 This effect is quantified by the evolution of the integral length scale $\mathcal{L}$, defined as

$$\mathcal{L} = \frac{\pi}{2K}\int_0^\infty \frac{E(k)}{k}dk \qquad (5)$$

where $K = \int_0^\infty E(k)dk$ is the total turbulent kinetic energy. The inset of Fig. 3 shows that $\mathcal{L}$ steadily increases in the post-reconnection regime, implying generation of large scale structures.

To explain the inverse energy transfer shown in Fig. 2, we look whether the reconnection triggers a chirality

imbalance. We decompose the incompressible Fourier modes of the normal fluid velocity into helical modes [42]:

$$\hat{\mathbf{v}}_n(\mathbf{k}) = \hat{\mathbf{v}}_n^+(\mathbf{k}) + \hat{\mathbf{v}}_n^-(\mathbf{k}) = v_n^+(\mathbf{k})\mathbf{h}^+(\mathbf{k}) + v_n^-(\mathbf{k})\mathbf{h}^-(\mathbf{k}), \tag{6}$$

where $\mathbf{h}^\pm(\mathbf{k})$ are the two eigenvectors of the curl operator, *i.e.* $i\mathbf{k} \times \mathbf{h}^\pm(\mathbf{k}) = \pm k\mathbf{h}^\pm(\mathbf{k})$. Similarly, we decompose the Fourier of the transverse mutual friction force: $\hat{\mathbf{F}}_{ns}^\perp = f^+\mathbf{h}^+ + f^-\mathbf{h}^-$ (the Fourier modes of $\mathbf{F}_{ns}$ parallel to the wavemumber $\mathbf{k}$ do not play any role in the time evolution of $\mathbf{v}_n$ due to the incompressible constraint). The spectral energy densities corresponding to the helical modes are $E^\pm(\mathbf{k}) = (1/2)|v_n^\pm(\mathbf{k})|^2$, the total spectral density being $E(\mathbf{k}) = E^+(\mathbf{k}) + E^-(\mathbf{k})$. Similarly the spectral helicity density is

$$\begin{aligned} H(\mathbf{k}) &= (1/2)\hat{\mathbf{v}}_n(\mathbf{k})\cdot\hat{\boldsymbol{\omega}}_n^*(\mathbf{k}) = \\ &= kE^+(\mathbf{k}) - kE^-(\mathbf{k}) = H^+(\mathbf{k}) - H^-(\mathbf{k}), \end{aligned} \tag{7}$$

where $\boldsymbol{\omega}_n$ is the normal fluid vorticity, the star indicates complex conjugate and $H^\pm$ is the helicity contribution of each separate helical mode. The rate of change $I^\pm(\mathbf{k})$ of the energies $E^\pm(\mathbf{k})$ arising from the mutual friction is proportional to the corresponding helical coefficients $f^\pm$, *i.e.* $I^\pm(\mathbf{k}) = \mathrm{Re}[f^\pm(v_n^\pm)^*]/\rho_n$, and the related signed helicity injection is $I_H^\pm(\mathbf{k}) = k\mathrm{Re}[f^\pm(v_n^\pm)^*]/\rho_n$.

A chiral imbalance occurs if the mutual friction force is helical, *i.e.* if the ratio $|f^+|^2/|f^-|^2 \neq 1$. In Fig. 4, we show the spectra of $|f^+|^2/|f^-|^2$, before, during and after the reconnection for both temperatures. It is apparent that during and after the reconnection, the mutual friction force is chiral, injecting more positive helicity than negative helicity. As a result, the ratio $\mathcal{H}^+/\mathcal{H}^-$ (reported in the inset of Fig. 4), where $\mathcal{H}^\pm(t) = \int H^\pm(\mathbf{k},t)d\mathbf{k}$), increases significantly at reconnection and remains larger than unity even at later times, indicating that the flow is chiral. We conclude that the reconnection triggers indeed a chiral imbalance.

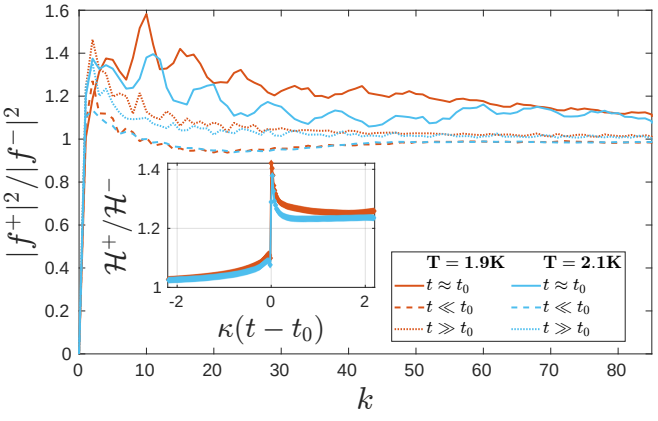

FIG. 4: The ratio of the projected helical mutual friction modes $f^+(k)$ and $f^-(k)$ at different times and temperatures as in Fig. 2

.

In conclusion, the reconnection of quantum vortices in the two-fluid regime ($T \gtrsim 1.5$K) not only injects punctuated energy in the normal fluid [43], but also triggers in the normal fluid a transfer of kinetic energy towards the large scales. This inverse energy transfer arises from the fact that the mutual friction force (injecting energy and helicity in the normal fluid) is helical, as Kelvin waves develop on the vortices. The helical character of the mutual friction produces a chiral imbalance in the normal fluid, driving this inverse cascade as previously observed in turbulent Navier-Stokes flows [28, 31]. Our findings have profound implications for the nature of finite temperature superfluid turbulence and motivate a detailed studied of fully coupled quantum turbulence to understand how energy transfer and dissipation is augmented by vortex reconnections.

G.K. was supported by the Agence Nationale de la Recherche through the project the project QuantumVIW ANR-23-CE30-0024-02. This work has been also supported by the French government, through the UCAJEDI Investments in the Future project managed by the National Research Agency (ANR) with the reference number ANR-15-IDEX-01. P.Z.S. acknowledges the financial support of the UCA "visiting doctoral student program" on complex systems. Computations were carried out at the Mésocentre SIGAMM hosted at the Observatoire de la Côte d'Azur.

[1] U. Frisch, *Turbulence: The Legacy of A. N. Kolmogorov* (1995).
[2] V. M. Canuto and J. Christensen-Dalsgaard, Turbulence in astrophysics: stars, Ann. Rev. Fluid Mech. **30**, 167 (1998).
[3] C. F. Barenghi, H. A. J. Middleton-Spencer, L. Galantucci, and N. G. Parker, Types of quantum turbulence, AVS Quantum Sci. **5**, 025601 (2023).
[4] C. F. Barenghi, L. Skrbek, and K. R. Sreenivasan, *Quantum Turbulence* (Cambridge University Press, 2023).
[5] L. F. Richardson, *Weather Prediction by Numerical Process* (University Press, 1922).
[6] A. Kolmogorov, The local structure of turbulence in an incompressible viscous fluid for very large Reynolds numbers, Dokl. Akad. Nauk. SSSR **30**, 301 (1941).
[7] R. Kraichnan, Inertial ranges in two-dimensional turbulence, Phys. Fluids **10**, 1417 (1967).
[8] G. Boffetta and R. E. Ecke, Two-dimensional turbulence, Ann. Rev. Fluid Mech. **44**, 427 (2012).
[9] G. Boffetta and S. Musacchio, Evidence for the double cascade scenario in two-dimensional turbulence, Phys. Rev. E **82**, 016307 (2010).
[10] J. Laurie, G. Boffetta, G. Falkovich, I. Kolokolov, and V. Lebedev, Universal profile of the vortex condensate in two-dimensional turbulence, Phys. Rev. Lett. **113**,

254503 (2014).
[11] L. Tisza, Transport phenomena in helium II, Nature **141**, 913 (1938).
[12] L. Landau, On the theory of superfluidity, Phys. Rev. **75**, 884 (1949).
[13] L. Skrbek and K. R. Sreenivasan, Developed quantum turbulence and its decay, Phys. Fluids **24**, 011301 (2012).
[14] B. Jackson, N. P. Proukakis, C. F. Barenghi, and E. Zaremba, Finite-temperature vortex dynamics in bose-einstein condensates, Phys. Rev. A **79**, 053615 (2009).
[15] H. E. Hall and W. F. Vinen, The rotation of liquid helium II. i. experiments on the propagation of secound sound in uniformly rotating helium II, Proc. R. Soc. London A **238**, 204 (1956).
[16] H. E. Hall and W. F. Vinen, The rotation of liquid helium II. ii. the theory of mutual friction in uniformly rotating helium II, Proc. R. Soc. London A **238**, 215 (1956).
[17] J. Maurer and P. Tabeling, Local investigation of superfluid turbulence, Europhys. Lett. **43**, 29 (1998).
[18] J. Salort, C. Baudet, B. Castaing, B. Chabaud, F. Daviaud, T. Didelot, P. Diribarne, B. Dubrulle, Y. Gagne, F. Gauthier, A. Girard, B. Hébral, R. B., P. Thibault, and P.-E. Roche, Turbulent velocity spectra in superfluid flows, Phys. Fluids **22** (2010).
[19] A. W. Baggaley, L. K. Sherwin, C. F. Barenghi, and Y. A. Sergeev, Thermally and mechanically driven quantum turbulence in helium II, Phys. Rev. B **86**, 104501 (2012).
[20] L. K. Sherwin-Robson, C. F. Barenghi, and A. W. Baggaley, Local and nonlocal dynamics in superfluid turbulence, Phys. Rev. B **91**, 104517 (2015).
[21] H. A. J. Middleton-Spencer, A. D. G. Orozco, L. Galantucci, M. Moreno, N. G. Parker, L. A. Machado, V. S. Bagnato, and C. F. Barenghi, Evidence of strong quantum turbulence in Bose-Einstein condensates, Phys. Rev. Research **5**, 043081 (2022).
[22] A. S. Bradley and B. P. Anderson, Energy spectra of vortex distributions in two-dimensional quantum turbulence, Phys. Rev. X **2**, 041001 (2012).
[23] M. T. Reeves, T. P. Billam, B. P. Anderson, and A. S. Bradley, Inverse energy cascade in forced two-dimensional quantum turbulence, Phys. Rev. Lett. **110**, 104501 (2013).
[24] T. Simula, M. J. Davis, and K. Helmerson, Emergence of order from turbulence in an isolated planar superfluid, Phys. Rev. Lett. **113**, 165302 (2014).
[25] S. P. Johnstone, A. J. Groszek, P. T. Starkey, C. J. Billington, T. P. Simula, and K. Helmerson, Evolution of large-scale flow from turbulence in a two-dimensional superfluid, Science **364**, 1267 (2019).
[26] G. Gauthier, M. T. Reeves, X. Yu, A. S. Bradley, M. A. Baker, T. A. Bell, H. Rubinsztein-Dunlop, M. J. Davis, and T. W. Neely, Giant vortex clusters in a two-dimensional quantum fluid, Science **364**, 1264 (2019).
[27] H. K. Moffatt, The degree of knottedness of tangled vortex lines, J. Fluid Mech. **36**, 7 (1969).
[28] L. Biferale, S. Musacchio, and F. Toschi, Inverse energy cascade in three-dimensional isotropic turbulence, Phys. Rev. Lett. **108**, 164501 (2012).
[29] L. Biferale, S. Musacchio, and F. Toschi, Split energy–helicity cascades in three-dimensional homogeneous and isotropic turbulence, J. Fluid Mech. **730**, 309–327 (2013).
[30] G. Sahoo, A. Alexakis, and L. Biferale, Discontinuous transition from direct to inverse cascade in three-dimensional turbulence, Phys. Rev. Lett. **118**, 164501 (2017).
[31] F. Plunian, A. Teimurazov, R. Stepanov, and M. K. Verma, Inverse cascade of energy in helical turbulence, J. Fluid Mech. **895**, A13 (2020).
[32] J. Koplik and H. Levine, Vortex reconnection in superfluid helium, Phys. Rev. Lett. **71**, 1375 (1993).
[33] G. P. Bewley, M. S. Paoletti, K. R. Sreenivasan, and D. P. Lathrop, Characterization of reconnecting vortices in superfluid helium, Proc. Natl. Acad. Sci. USA **105**, 13707 (2008).
[34] C. Rorai, J. Skipper, R. Kerr, and K. Sreenivasan, Approach and separation of quantum vortices with balanced cores, J. Fluid Mech. **808**, 641 (2016).
[35] S. Serafini, L. Galantucci, E. Iseni, T. Bienaime, R. Bisset, C. F. Barenghi, F. Dalfovo, G. Lamporesi, and G. Ferrari, Vortex reconnections and rebounds in trapped atomic Bose-Einstein condensates, Phys. Rev. X **7**, 021031 (2017).
[36] L. Galantucci, A. W. Baggaley, N. G. Parker, and C. F. Barenghi, Crossover from interaction to driven regimes in quantum vortex reconnections, Proc. Natl. Acad. Sci. USA **116**, 12204 (2019).
[37] A. Villois, D. Proment, and G. Krstulovic, Irreversible dynamics of vortex reconnections in quantum fluids, Phys. Rev. Lett. **125**, 164501 (2020).
[38] L. Galantucci, A. W. Baggaley, C. F. Barenghi, and G. Krstulovic, A new self-consistent approach of quantum turbulence in superfluid helium, Eur. Phys. J. Plus **135**, 547 (2020).
[39] See supplementary materials.
[40] P. Gualtieri, F. Picano, G. Sardina, and C. M. Casciola, Exact regularized point particle method for multiphase flows in the two-way coupling regime, J. Fluid Mech. **773**, 520 (2015).
[41] P. Gualtieri, F. Battista, and C. M. Casciola, Turbulence modulation in heavy-loaded suspensions of tiny particles, Phys. Rev. Fluids **2**, 034304 (2017).
[42] F. Waleffe, The nature of triad interactions in homogeneous turbulence, Phys. Fluids A **4**, 350 (1992).
[43] P. Z. Stasiak, Y. Xing, Y. Alihosseini, C. F. Barenghi, A. W. Baggaley, W. Guo, L. Galantucci, and G. Krstulovic, Quantum vortex reconnections, arXiv , 2411.08942 (2024).